Eur Biophys J (2007) 36:1083–1094
DOI 10.1007/s00249-007-0212-9

ORIGINAL PAPER

H2A and H2B tails are essential to properly reconstitute nucleosome core particles

Aurélie Bertin · Dominique Durand · Madalena Renouard · Françoise Livolant · Stéphanie Mangenot

Received: 19 February 2007 / Revised: 25 June 2007 / Accepted: 24 July 2007 / Published online: 19 September 2007

Abstract The conformation of recombinant Nucleosome Core Particles (NCPs) lacking H2A and H2B histone tails (gH2AgH2B) are studied. The migration of these particles in acrylamide native gels is slowed down compared to intact reconstituted NCPs. gH2AgH2B NCPs are also much more sensitive to nuclease digestion than intact NCPs. Small angle X-ray scattering (SAXS) experiments point out that the absence of H2A and H2B tails produces small but significant conformational changes of the octamers conformation (without wrapped DNA), whereas gH2AgH2B NCP conformations are significantly altered. A separation of about 25–30 bp from the core could account for the experimental curves, but other types of DNA superhelix deformation cannot be excluded. The distorted gH2AgH2B octamer may not allow the correct winding of DNA around the core. The absence of the H2A and H2B tails would further prevent the secondary sliding of the DNA around the core and therefore impedes the stabilisation of the particle. Cryo-electron microscopy on the same particles also shows a detachment of DNA portions from the particle core. The effect is even stronger because the vitrification of the samples worsens the instability of gH2AgH2B NCPs.

A. Bertin · M. Renouard · F. Livolant · S. Mangenot (✉)
Laboratoire de Physique des Solides, CNRS UMR 8502,
Université Paris-Sud, 91405 Orsay Cedex, France
e-mail: mangenot@lps.u-psud.fr

D. Durand
IBBMC, CNRS UMR 8619, Université Paris-Sud,
91405 Orsay Cedex, France

Present Address:
A. Bertin
Nogales Laboratory, Molecular and Cellular Biology
Department, University of California,
Berkeley, CA 94720-3200, USA

Keywords Nucleosome · Histone tails · SAXS · Chromatin

Introduction

The nucleosome core particle (NCP) has been precisely described, at high resolution (Luger et al. 1997a; Davey et al. 2002). Two superhelical turns of DNA [146–147 base pairs (bp)] are wrapped around a disk-shaped protein octamer containing two copies of four different histones (H2A, H2B, H3 and H4). The crystallographic data at 1.9 Å resolution (Davey et al. 2002) display the histones-DNA contacts and the location of unstructured N- and C-terminal portions of three histones. Those unstructured portions, commonly called histone tails, contain a high proportion of basic residues (lysines and arginines). At moderate concentrations of monovalent salts (150–300 mM) tail domains are mobile and can extend beyond the particle core (Smith and Rill 1989; Mangenot et al. 2002; Bertin et al. 2004).

Histone tails are known to be involved in many biological processes. They are necessary for ATPase activity of remodeling factors such as ISWI and NURF (Clapier et al. 2001; Hamiche et al. 2001) and nucleosomal DNA transcription (Protacio et al. 2000; Yang et al. 2005). Subject to post-translational modifications, histone tails have the potential to modulate intra and inter nucleosomal interactions (Cosgrove and Wolberger 2005). Indeed, hyper-acetylated chromatin fibers present a low degree of compaction (Pollard et al. 1999) related, in vivo, with the activation of the transcription machinery, whereas this activity is repressed on deacetylated chromatin (Cheung et al. 2000). Acetylation of the lysine residues induces neutralization of the lysine positive charges. As a

consequence, tailless chromatin and nucleosomes are often used to mimic the effect of acetylation. Nucleosome oligomers deprived of some of the histone tails remain indeed only partially condensed as compared with native ones, upon divalent cation addition (Garcia-Ramirez et al. 1992; Fletcher and Hansen 1995; Krajewski and Ausio 1996; Tse and Hansen 1997; Dorigo et al. 2003; Gordon et al. 2005).

In order to determine the role of histone tails, they can be completely or specifically removed either by enzymatic digestion or by reconstitution using recombinant histones deprived of their terminal extensions. Upon those tail deletions, several authors have shown that the global NCP conformation remains rather unaffected (Ausio and van Holde 1989; Dumuis-Kervabon et al. 1986). However, tailless particles are more sensitive to thermal (Ausio and van Holde 1989) and mechanical stress (Brower-Toland et al. 2005).

The use of intact recombinant histones and DNA has proven to be of great interest to produce perfectly monodisperse particles and yield nucleosome high resolution structures (Luger et al. 1997a, b). Using salt gradient reconstitution any tail combination can be theoretically obtained. However, we have noticed that the absence of both H2A and H2B terminal extensions is critical for the histone octamer to be properly reconstituted onto *Lytechinus variegatus* 5S 146 bp DNA fragments. Digestion with micrococcal nuclease, cryoelectron microscopy and small-angle X-ray scattering (SAXS) are used here to analyze the conformational disruptions occurring for NCPs reconstituted using tail-depleted H2A and H2B histones (designated as gH2AgH2B, where g denotes globular histones).

Materials and methods

Preparation of octamers and nucleosome core particles

Recombinant nucleosome core particles were prepared according to Dyer et al. (2004). A detailed description of the protocol is given in Bertin et al. (2007). Four types of histone octamers were reconstituted: intact, gH3gH4 (deprived of their H3 and H4 tails), gH2AgH2B (without H2A and H2B tails) and without any tails (Table 1). The tailless histones have been designed by Luger et al. (1997b). Intact or "trypsin-resistant" globular recombinant *Xenopus laevis* histones were expressed separately in BL21DE3-pLysS *Escherichia coli*. The plasmids for expressing intact or globular histones have been kindly provided by K. Luger. Histones were purified by size exclusion followed by ion-exchange chromatography, dialyzed against 5 mM β-mercaptoethanol in water, lyophilized, aliquoted and stored at –80°C. After solubilisation in denaturing buffer (7 M guanidinium hydrochloride, 10 mM DTT, 20 mM Tris–HCl, pH 8), a chosen combination of intact or globular histones were mixed in a stoechiometric ratio for a final histone concentration of 1 mg mL^{-1}. The mixture was dialyzed (Spectra-por, MW cut-off: 6,000–8,000) against a renaturation buffer (2 M NaCl, 5 mM DTT, 1 mM EDTA, 10 mM Tris–HCl, pH 8) at 4°C, concentrated up to 10 mg mL^{-1} and purified by size exclusion chromatography in the same buffer. β-mercaptoethanol adducts were detected on H3 and gH3 histones by mass spectrometry (data not shown). The adduct covalent bonds between cystein amino-acids and β-mercaptoethanol molecules were easily removed after 5 mM DTT addition. Consequently, DTT was chosen instead of β-mercaptoethanol, which improved significantly the octamer reconstitution.

Table 1 *Xenopus laevis* histone molecular mass determination using mass spectrometry

Histone	a.a. Sequence	Measured mass	Calculated mass
H2A	1–128	13,949.0	13,950.2
H2B	1–122	13,493.7	13,493.7
H3	1–135	15,272.3	15,270.9
H4	1–102	11,236.5	11,236.2
gH2A	13–117	11,739.2	11,739.2
gH2B	24–122	11,291.3	11,288.1
gH3	27–135	12,656.2	12,653.9
gH4	20–102	9,522.9	9,521.2

Measured masses were determined with a Maldi-TOF apparatus. Calculated masses were obtained from the web site: http://www.expasy.org/tools/peptide-mass.html after entering the histone sequences

To prepare recombinant nucleosome core particles, 146 bp DNA was prepared from a segment of the 5S RNA gene of *Lytechinus variegatus* (Richmond et al. 1988) and purified using an anion exchange chromatography column (DEAE-5PW, Tosohaas). Nucleosome core particle reconstitution was performed by mixing pure histone octamers and 5S 146 bp DNA in a DNA: histone octamer ratio of 1:1.2 in a high salt buffer (2 M KCl, 10 mM DTT, 0.5 mM EDTA, 10 mM Tris–HCl, pH 8). The solution was gradually dialyzed to a low salt buffer (0.25 M KCl, 5 mM DTT, 0.5 mM EDTA, 10 mM Tris–HCl, pH 8) at 4°C, further dialyzed for four more hours in the same buffer and equilibrated in TCS buffer (20 mM Tris–HCl, 1 mM EDTA, pH 7.6). Aggregates were removed by centrifugation during 20 min at 12,000*g*. NCPs were heated to 37°C to achieve DNA positioning around the histone core. After concentration by ultrafiltration up to 10 mg mL^{-1}, nucleosome core particle solutions were loaded on a 6%, 7.5 cm high nondenaturing polyacrylamide gels cast in a Bio-Rad Prep-cell apparatus. Pure NCP fractions were purified from free DNA, aggregates and partially unshifted NCPs by preparative gel electrophoresis performed at a constant power

of 10 W. Eluted fractions were immediately concentrated by ultrafiltration to prevent any nucleosome dissociation.

DNA sensitivity to micrococcal nuclease digestion

MNase digestions were performed at 37°C in a 10 mM Tris–HCl buffer, pH 8, containing 5 mM $CaCl_2$. NCP concentrations were adjusted to 0.16 mg mL^{-1}. Time course experiments were performed for a constant MNase concentration of 0.015 units per µg of NCPs and digestion times were varied from 0 to 16 min. Reactions were stopped on ice upon the addition of 5 mM EGTA and 1% SDS. Histones were finally digested using 5 µg of proteinase K per mg of NCPs at 37°C for 30 min. DNA fragments were analyzed by electrophoresis on 5% acrylamide gels.

Small angle X-ray scattering

Samples preparation for SAXS

Two sets of small angle X-ray scattering experiments were carried out on NCPs and histone octamers. Immediately after purification, NCPs were dialyzed against 10 mM Tris–HCl buffer, pH 7.6 containing 1 mM EDTA, 0.1 mM PMSF and 2 mM DTT. NCP concentrations were adjusted to be 8 mg mL^{-1}. Concentrations were assessed by UV-absorbance measurements. Various NaCl buffer solutions were prepared and added to dialyzed nucleosome core particle solutions to adjust final monovalent salt concentrations. Added NaCl solution concentrations never exceeded 300 mM to prevent any NCP dissociation. Monovalent salt concentrations C_s (including both $Tris^+$ and Na^+ ions) were 10, 25, 50, 100 and 150 mM. For each salt concentration, NCPs were diluted to 4, 2 and 1 mg mL^{-1}. Sample volumes were adjusted to 50 µL.

After histone octamer assembly and purification, octamers were concentrated using a Vivascience Vivaspin concentrator (10,000 MW cut-off) to 16 mg mL^{-1} and diluted to 8 and 4 mg mL^{-1} in the renaturation buffer. Prior to SAXS experiments, 4 mM of fresh DTT was added to the solution.

SAXS data collection

SAXS experiments on NCPs, were carried out on a commercially available small-angle X-ray camera (Nanostar, Brucker AXS) adapted to a rotating anode X-ray source (CuKα, $\lambda = 1.54$ Å). The experimental setup was optimized by Jan Skov Pedersen (University of Aarhus, Denmark) to obtain higher flux (Pedersen 2004). The instrument has an integrated vacuum in order to reduce background. The scattering vector range was 0.01 $Å^{-1} < q < 0.35$ $Å^{-1}$, where $q = 4\pi \sin\theta/\lambda$, with 2θ being the scattering angle. The sample to detector distance was 662 mm. Samples were enclosed into 2 mm diameter quartz capillaries directly inserted into vacuum. Measurements were performed at 5°C. Both buffers and samples were exposed during 7,200 s. Data were collected using a position-sensitive gas detector (HiSTAR). The SAXS data were azimuthally averaged, corrected for variations in detector efficiency and for spatial distortions. Measurements on buffers were used as backgrounds and were subtracted from the recorded integrated curves. Finally, the data were converted to absolute scale using the scattering from pure water as primary standard.

Experiments with octamers were carried out on the X33 beamline at the radiation synchrotron source located in the HASYLAB experimental hall (Hamburg, Germany) (http://www.emblhamburg.de/ExternalInfo/Research/Sax/beamline.html). A horizontal focusing triangular Si (111) monochromator was used to select the 1.5 Å wavelength. The detector was a MAR345 Image Plate detector. The sample to detector distance was set to 2.7 m corresponding to the scattering vector range 0.01 $Å^{-1} < q < 0.495$ $Å^{-1}$. Hundred microliter of the samples were placed in a flat cell with mica windows in which temperature was adjusted to 10°C. Two successive frames of 180 s each were recorded for NCPs and buffers. We carefully checked all frames to ensure that octamers were not damaged by the X-ray beam. The data were normalized to the intensity of the incident beam and processed to background subtraction using the standard procedures with the program package PRIMUS (Konarev et al. 2003).

SAXS data analysis

Considering noninteracting particles, the scattering intensity at low q values can be approximated by Guinier plot ($\ln I(q) = \ln I(0) - q^2R_g^2/3$), readily yields the value of the radius of gyration of the particles R_g and the value of the intensity at null scattering angle $I(0)$. This approximation can be used in the range $qR_g < 1.3$.

The distance distribution function $P(r)$ corresponding to the distribution of distances between two volume elements inside one particle, is the Fourier transform of the scattering intensity $I(q)$. It was determined using the program GNOM (Svergun 1992). $P(r)$ is equal to zero for distances larger than the maximal extension D_{max} of the particle. This function provides an alternative estimate of the radius of gyration.

Scattering intensities were computed from the atomic coordinates of the crystal structure of NCP (PDB entry 1KX5) using the program CRYSOL (Svergun et al. 1995).

Structures were modified using PyMOL that creates new PDB files. Computed scattering curves were fitted and compared with experimental data. The rigid-body modelling program SASREF (Petoukhov and Svergun 2005) is used to find the position of the tails in the octamers. In the program SASREF, a simulated annealing protocol is employed to construct an interconnected ensemble of subunits without steric clashes using their high-resolution structures. The minimization procedure starts from an arbitrary arrangement of subunits. In our case, the starting structure of the subunits (core and tails) was obtained from the crystallographic structure 1KX5. The discrepancy between the calculated and the experimental scattering profiles is then minimized. The goodness of fit was characterized by the χ parameter: $\chi^2 = \frac{1}{N-1}\sum_j \left[\frac{I_{\exp}(q_j) - cI_{\text{calc}}(q_j)}{\sigma(q_j)}\right]^2$ where N is the number of experimental points, c is a scaling factor, and $I_{\exp}(q_j)$, $I_{\text{calc}}(q_j)$ and $\sigma(q_j)$ are the experimental intensity, the calculated intensity and the experimental error at the scattering vector q_j, respectively.

Cryo-electron microscopy

NCPs in TE (10 mM Tris–HCl buffer, 1 mM EDTA, pH 7.6) were vitrified using a chamber designed and set up in the laboratory where both humidity and temperature can be controlled. A 4 µL drop of the NCP solution concentrated at 2.5 mg mL^{-1} was deposited onto a perforated carbon film mounted on a 200 mesh electron microscopy grid. The home-made carbon film hole dimensions are about 2 µm in diameter. Most of the drop was removed with a blotting filter paper and the residual thin films remaining within the holes were vitrified after immersion in liquid ethane using a guillotine-like frame. The specimen was then transferred using liquid nitrogen to a cryo-specimen holder and observed using a CM-12 Philips and a JEOL FEG-2010 electron microscope. Micrographs were recorded at 80 and 200 kV, respectively, under low-dose conditions at a magnification of 45,000 on SO-163 Kodak films. Micrographs were digitised using a film scanner (Super coolscan 8000 ED, Nikon) and their contrast was magnified with the image J software.

Results

Biochemical characterization of octamers and nucleosome core particles

Histone octamer characterization

The purity of the full length or tailless individual histones was checked by electrophoresis on SDS-Polyacrylamide gels (data not shown) and mass spectrometry experiments. Measured histone masses are in excellent agreement with theoretical masses calculated from the web site http://www.expasy.org/tools/peptide-mass.html using the protein sequences (Table 1). Protein composition of the four reconstituted octamers (intact, gH3gH4, gH2AgH2B and without any tail) was checked by SDS-PAGE (data not shown). The equal intensities of the four bands attest for the histones stoechiometry.

DNA positioning around the histone octamer

After salt gradient reconstitution, solutions contain multiple NCP populations due to multiple DNA positions around the octamer. For intact NCPs, three distinct bands are observed on nondenaturing acrylamide gels (Fig. 1a, Line 2). The lowest one, which migrates faster in the gel, corresponds to a configuration where DNA is centrally positioned around the histone octamer (Dong et al. 1990). The higher bands reveal particles in which DNA is asymmetrically positioned. One of the DNA entry/exit ends is protruding from the particle core, and slows down the NCP migration in the gel. DNA positioning around the core is sensitive to temperature. Heating the samples reduces the energy barrier that prevents DNA from reaching thermodynamic equilibrium and from being centrally positioned (Pennings et al. 1991; Meersseman et al. 1992).

In order to get a homogeneous centrally positioned batch of particles, samples were heated. For intact NCPs, DNA shift is complete after 8 min at 37°C, leading to the observation of one single band (Fig. 1a, line 1). The reconstitution of intact nucleosomes is very efficient using a histone:DNA molar ratio of 1.2:1 and no 146 bp free DNA is detected in our gels. For gH3gH4 NCPs, a unique NCP band was obtained after 60 min at 37°C (Fig. 1b, line 1) suggesting that a unique positioning of DNA was achieved around histone octamers. This positioning is probably central around the histone octamer since gH3gH4 NCPs migrate at the position of intact NCPs (Fig. 1d). The reconstitution is not completely efficient and a fraction of 146 bp DNA stays free in solution (bar in Fig. 1b). For reconstituted gH2AgH2B NCPs, at least two NCP bands are observed prior to thermal heating (Fig. 1c, line 2) in addition to the intense 146 bp free DNA band. After 45 min heating at 37°C, a unique NCP band is usually obtained. However, a purified solution showing only one band turns back to two bands after a few days (Fig. 1e, line 1), leading to the conclusion that gH2AgH2B NCPs are polymorphic and less stable. DNA is probably able to move spontaneously from one position to an other around the histone core. NCPs with all tails missing (gH2AgH2BgH3gH4) were also reconstituted into

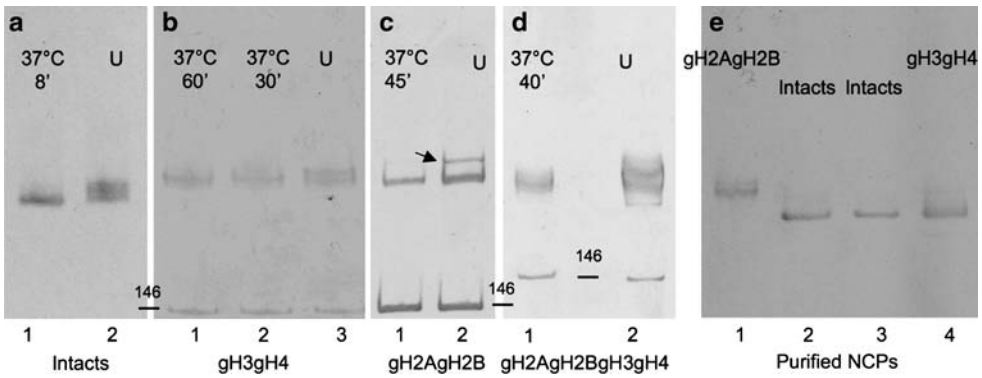

Fig. 1 Positioning of DNA around histone octamers upon heating at 37°C by comparison with unheated samples (*U*). For Intact NCPs (**a**) and gH3gH4 NCPs (**b**), DNA is shifted to a unique position after 8 and 60 min, respectively. For gH2AgH2B NCPs (**c**), the upper band, marked with the *arrow*, disappears after heating. Heating has no effect on tailless NCPs migration (**d**). The *bar* points to the free 146 bp DNA. Electrophoreses are run for different times in 5% nondenaturing polyacrylamide gels and stained with ethidium bromide. (**e**) Purified samples, devoid of aggregates and free DNA, are used for SAXS experiments. gH2AgH2B NCPs migrate more slowly than intact and gH3gH4 NCPs in a 5% non denaturing polyacrylamide gel

particles that migrate as a single band after 40 min heating at 37°C (Fig. 1d). These NCPs migrate quite similarly to the gH2AgH2B NCPs (not shown) but both migrate well above the gH3gH4 and intact NCPs.

Aggregates and free DNA are eliminated by preparative electrophoresis, and the quality of the samples is checked by PAGE on 5% gels (Fig. 1e). When compared with intact and gH3gH4, the gH2AgH2B NCPs migrate significantly more slowly (Fig. 1e). This particular behavior emphasizes conformational particularities of the gH2AgH2B NCPs. The conformation of the particle is different from the canonical structure of the intact NCP with either an extended global conformation and/or DNA ends extending outside of the particle, slowing down their migration in the gel.

Reconstitution yields

The efficiency of NCPs reconstitution highly depends on the presence of the histone tails. Important aggregation occurs with globular histones compared to intact full-length proteins. For tailless particles, aggregation occurs whatever the DNA:histone molar ratio is. These aggregates made of both DNA and proteins were removed by centrifugation. Yields are also much higher for intact NCPs because there is almost no free DNA left in the solution (Fig. 1a), compared to gH3gH4, gH2AgH2B and tailless NCPs where the free DNA band is noticeable (Fig. 1b–d). Consequently, reconstitution yields vary between 50 and 80% for intact NCPs, equal 50% for gH3gH4 and only about 30% for gH2AgH2B NCPs. For tailless NCPs, this yield is below 10%. Consequently, production of tailless NCPs in sufficient quantity to perform SAXS or cryo-EM experiments was never achieved despite many attempts.

DNA sensitivity to micrococcal nuclease digestions

Nucleosomal DNA is known to be protected from *Micrococcal* nuclease digestion in intact NCPs (Noll 1974). To determine the possible role of histone tails on the NCP conformation, we have performed MNase digestion experiments with 0.015 units MNase per μg of NCPs on intact, gH3gH4 and gH2AgH2B NCPs (Fig. 2). DNA from intact NCPs was not affected after 4 min incubation with MNase. For the longest digestion time (8 and 16 min), a lower band can be perceived that is about 15–20 bp lower than the 146 bp of the 5S DNA. DNA appears to be more sensitive to MNase digestion in gH3gH4 NCPs. DNA is already partially digested into DNA pieces of approximately 130 and 115 bp after 2 min of incubation with nucleases. After 16 min digestion, 146 bp DNA fragments and much shorter DNA pieces (105 ± 5 bp) are still remaining. Nucleosomal DNA wrapped around gH2AgH2B octamers is significantly more affected by MNase activity. After 8 min digestion, we observe the apparition of at least two bands corresponding to shorter fragments of approximately 135 and 120 bp and the disappearance of 146 bp DNA fragments. A 110 bp fragments appear after 16 min digestion. These fragments correspond to transient steps of protection of the nucleosomal DNA. Nevertheless, for gH2AgH2B and also for gH3gH4 the sum of intensities of all bands is much lower than the intensity of the non-digested 146 bp DNA fragments. As the same amount of DNA was deposited in all wells, a fraction of the 146 bp DNA has been completely digested into small fragments that are eluted from the gels.

gH2AgH2B NCPs are therefore much more sensitive to MNase digestion than gH3gH4 and to a larger extent than intact NCPs since only approximately 135 and 120 bp DNA are sequentially and transiently protected against MNase digestion.

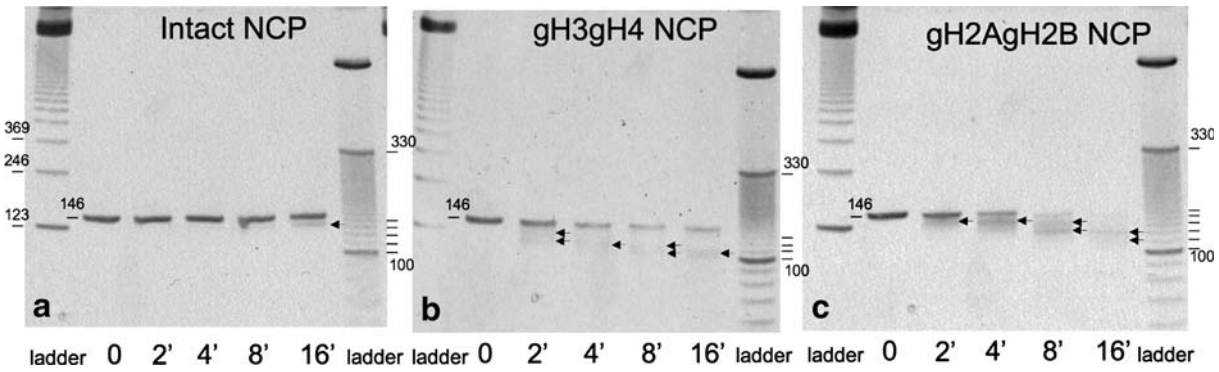

Fig. 2 Micrococcal nuclease digestion time course experiments of intact (**a**), gH3gH4 (**b**) and gH2AgH2B (**c**) recombinant NCPs. NCP concentration was fixed to 0.16 mg mL^{-1} and 0.015 units of MNase per μg of NCPs were used. Digestion times varied from 0 to 16 min. Deproteinized samples were analyzed by 5% polyacrylamide gel electrophoresis, stained with ethidium bromide. DNA ladders, 123 and 10 pb (Invitrogen), were used as markers. DNA size markers are given

We have shown previously that gH2AgH2B NCPs migration in gels is significantly slowed down compared to intact NCPs (Fig. 1e). One could therefore argue that DNA is not symmetrically positioned on those NCPs and that protruding DNA ends would therefore be preferentially digested by MNase. Either one or both end could be slightly detached from the particle core.

Lower stability of gH2AgH2B upon vitrification in thin cryo-EM films

Intact and gH2AgH2B NCPs were vitrified in thin films to be imaged by cryo-electron microscopy. Intact NCPs stay undamaged and were imaged under low dose conditions in TE buffer (Fig. 3b). In contrast, gH2AgH2B NCPs happened to be destabilized during this process. In the thinnest regions of the films, large amounts of free DNA are observed, revealing that part of the NCPs are fully dissociated (data not shown). In thicker samples, long filaments are aligned perpendicularly to the carbon holes limits. Some of them are terminated by a roundshaped domain (Fig. 3a, arrow). Those filaments correspond to DNA fragments decorated with free histones. Since intact NCPs are not modified using the same preparation protocol, this method reveals a lower stability of gH2AgH2B particles compared to the intact ones. It is unlikely that this destabilization may be a consequence of the vitrification process. We rather suspect the surface tension forces occurring within the film prior to the vitrification step to be responsible for this destabilization and/or dissociation of the gH2AgH2B core particles.

SAXS experiments

SAXS experiments were carried out on intact, gH3gH4 and gH2AgH2B NCPs after thermal heating at 37°C. Curves recorded for intact and gH3gH4 NCPs at 4 mg mL^{-1} NCP concentrations and in 25 mM monovalent salt are very much alike (Fig. 4) (detailed in Bertin et al. 2007). At any particle and salt concentrations, the second minimum around 0.14 $Å^{-1}$ is not as deep for gH3gH4 NCPs and it is barely perceptible for gH2AgH2B. Form factors are thus very different for gH2AgH2B NCPs compared to intact and gH3gH4 particles, implying that gH2AgH2B NCPs display conformational distinctive features.

Since gH2AgH2B NCPS present a lower mobility in polyacrylamide gels, a higher sensitivity of nucleosomal

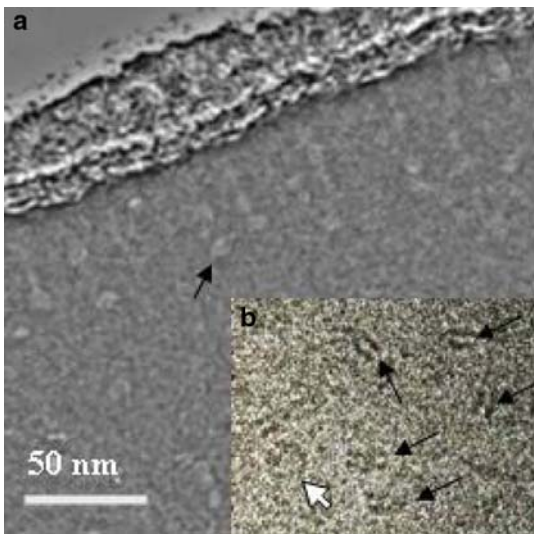

Fig. 3 Cryo-electron microscopy of gH2AgH2B (*a*) and intact recombinant NCPs (*b*) in TE buffer under low electron dose conditions. gH2AgH2B NCPs are destabilized upon vitrification in thin films. They appear as elongated thick filaments aligned perpendicular to the limit of the carbon hole and decorated by proteins at their extremity (*arrow*) and/or along their length. In the same conditions, intact NCPs present their characteristic shape as seen in *top view* (*white arrow*) and in *side views* (*black arrows*). Micrographs are taken in a CM-12 Philips microscope at 80 kV (*a*) and in a FEG JEM-2010 microscope at 200 kV (*b*)

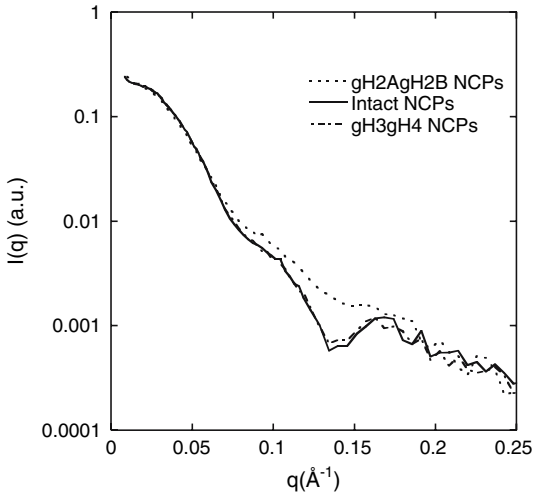

Fig. 4 Small angle X-ray scattering curves obtained at a particle concentration of 4 mg mL^{-1} in a 25 mM monovalent salt solution. Intact (*solid line*), gH3gH4 (*dashed line*) and gH2AgH2B (*dotted line*) NCPs are compared

DNA to micrococcal nuclease activity, a lower stability as revealed by cryoEM and a significantly different SAXS scattering profile, one can hypothesize that the absence of H2A and H2B tails prevents the reconstitution of a NCP in its canonical conformation. The question is to know whether these H2A and H2B tails are required: (a) for the assembly of the octamer into its canonical form, (b) for the wrapping of the DNA and its correct positioning around the histone octamer or (c) at these two steps of the NCP assembly. SAXS experiments were thus performed on intact, gH3gH4 and gH2AgH2B histone octamers (with no wrapped DNA). SAXS curves were measured for three particle concentrations, 4, 8 and 16 mg mL^{-1} in the renaturation buffer (2 M NaCl, 5 mM DTT, 1 mM EDTA, 10 mM Tris–HCl, pH 8). For intact and gH3gH4 octamers the curves corresponding to the three concentrations are identical. The value obtained for $I(0)$ by fitting $I(q)$ at low q using the Guinier law is in good agreement with the theoretical value (see the expression in Bertin et al. 2007). It indicates that intact and gH3gH4 octamers solutions are free of aggregation whatever the concentration. gH2AgH2B solutions concentrated at 4 and 8 mg mL^{-1} produce also identical curves and show the previous behaviour concerning $I(0)$. On the contrary, the shape at low q of the 16 mg mL^{-1} solution indicates a small percentage of oligomers. For this reason, all the conformational analyses were performed using the curve recorded at 16 mg mL^{-1} for intact and gH3gH4 octamers and 8 mg mL^{-1} for gH2AgH2B octamers. The curves are presented on Fig. 5a. These graphs display the form factors of the three types of octamers. These form factors are nearly identical for intact and gH3gH4 octamers, whereas it is slightly different for the gH2AgH2B octamers as it can be seen from the R_g and D_{max} values (Table 2) and from the shapes of the distance distribution function $P(r)$ (Fig. 6).

R_g is found to be nearly identical for intact and gH3gH4 octamers in the range 32.5–33 Å, whereas for gH2AgH2B octamers, this value is slightly higher and equal to about 36 Å. The $P(r)$ distribution shows larger extension of the particle for gH2AgH2B compared with the intact and the

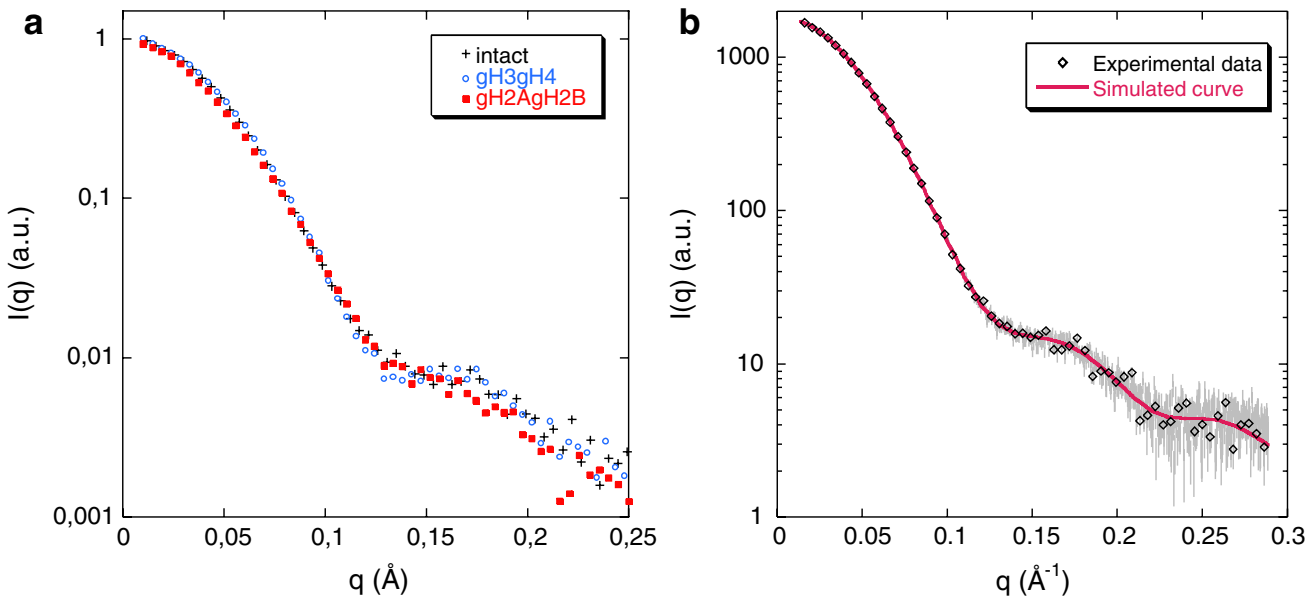

Fig. 5 **a** SAXS data recorded at 16 mg mL^{-1} for intact and gH3gH4 octamers and at 8 mg mL^{-1} for gH2AgH2B octamers in the renaturation buffer (2 M NaCl, 5 mM DTT, 1 mM EDTA, 10 mM Tris–HCl, pH 8). **b** Comparison of simulated and experimental scattering intensities and error bars of intact octamers. Simulated curves were obtained with SASREF program

Table 2 Experimental values of the radius of gyration calculated from the Guinier's approximation, R_g (Guinier) and from the $P(r)$ function, R_g ($P(r)$)

Sample	Intact octamers (Å)	gH3gH4 octamers (Å)	gH2AgH2B octamers (Å)
R_g (Guinier) (Å)	32.5 ± 0.2	32.6 ± 0.2	35.7 ± 0.3
R_g ($P(r)$) (Å)	33.3 ± 0.2	33.0 ± 0.2	37.2 ± 0.2
D_{max}	115 ± 5	125 ± 5	140 ± 5

The values of the maximum extension of the particle, D_{max}, are also indicated

gH3gH4 octamers. This change is reflected in the values of the maximum extension of the particle, D_{max} (Fig. 6, Table 2), which is equal to approximately 120 ± 5 Å for intact and gH3gH4 octamers and increases by about 20 Å for the gH2AgH2B NCPs. The values of the radius of gyration deduced from the $P(r)$ functions are also displayed on Table 2. Within the errors bars, these values are nearly identical to the values of R_g calculated with the Guinier's approximation.

In order to perform any in-depth analysis of the octamer conformations, we compared our experimental scattering curve of the intact octamer with the simulated one. Recent crystallographic data have been obtained on the conformation of intact octamers (Chantalat et al. 2003) (PDB entry 1HQ3) but histone tails were not localized in this structure, whereas they were all present in the NCP structure (Davey et al. 2002) (PDB entry 1KX5). The histone core conformations of the two structures are superimposed and their scattering intensities, calculated with CRYSOL are

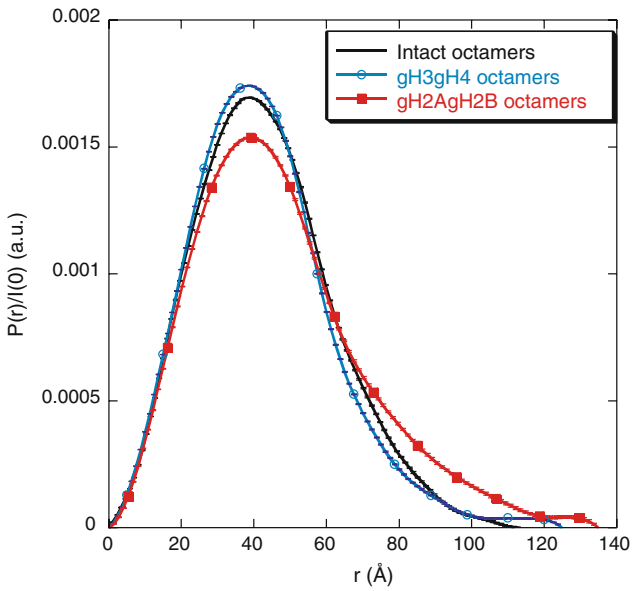

Fig. 6 Comparison of the distance distribution functions $P(r)$ normalized by the scattering intensity extrapolated at $q = 0$ for the intact, gH3gH4 and gH2AgH2B octamers

identical. For this reason, all the conformational analyses were performed with the histone octamer structure of the NCP crystal (PDB entry 1KX5). In this structure, the first amino acids extending from the globular core follow a straight path through DNA. This configuration does not probably reflect the octamer tails configuration which should be free to move around the histone core. We thus used the SASREF program (Petoukhov and Svergun 2005), to move the tails with respect to the histone core. The experimental and simulated curves are displayed on Fig. 5 b. The agreement between the two curves is excellent on the whole q range ($\chi^2 = 1.5$). We observe that in the configuration resulting from the simulation, the tails were found to be partially folded onto the histone core.

The same procedure has been used to simulate the gH3gH4 and the gH2AgH2B octamer experimental curves. In the first case, a good agreement between experimental and simulated curves is obtained when tails H2A and H2B are moved away from the core ($\chi^2 = 1.6$). For the gH2AgH2B octamers, no accurate fit has been obtained with the octamers conformation extracted from the NCP crystallographic structure (The best χ^2 is found to be equal to 2.31).

Discussion

Octamers conformation

As displayed on Fig. 5b, the experimental scattering intensity of the intact octamer is in perfect agreement with the calculated intensity of a core octamer extracted from the NCP crystallographic data, with tails partially folded. Tails are found to be closer to the core than in the NCP structure because of the absence of interaction with DNA. The scattering curves and the radii of gyration of intact and gH3gH4 octamers are nearly identical (Fig. 5a, Table 2), leading to the conclusion that both octamers conformations are very much alike. However, the D_{max} value is slightly higher, by approximately 10 Å, for gH3gH4 NCPs. This increase could be due to a slightly larger extension of the H2A–H2B histone tails as observed with the SASREF simulations, itself due to a small conformational change of the histone core. However, these differences are weak. On the contrary, the gH2AgH2B octamer shows significant differences with the intact octamer (Figs. 5a, 6, Table 2). It is clearly visible on the $P(r)$ curves. The values of the radius of gyration and the maximum extension D_{max} are increased by, respectively, 3 and 25 Å as compared with the intact octamers.

Without H2A histone tails, it has been shown that H2A–H2B histone dimers have a lower affinity for H3–H4 histone tetramers (Eickbush et al. 1988). Consequently,

histone octamers containing tailless H2A are expected to be less compact than intact octamers. The absence of H2A and H2B histone terminal extensions affects H2A–H2B dimer structure and stability (Placek and Gloss 2002). Without those tails, the α-helical content of the dimer is actually altered. However, the thermodynamic stability of H2A–H2B dimers and H3–H4 tetramers does not seem to be altered (Karantza et al. 2001).

NCPs conformation

Considering NCPs, conformations of gH3gH4 and intact NCPs are very close. Nevertheless, the conformation of gH3gH4 is slightly more opened since the form factor second minimum is not as deep as for intact NCPs. This slight conformational dissimilarity is detailed in another article (Bertin et al. 2007) and accounts for the MNase enhanced sensitivity. Differences in the scattering intensities observed between intact and gH2AgH2B NCPs (Fig. 4) are more significant than the differences between the corresponding octamers. To evaluate the balance of histones and DNA contributions to the scattering data, the scattering intensities of intact histone octamers, wrapped DNA and intact NCPs are compared (Fig. 7). Calculations were made with the program CRYSOL using the PDB file 1KX5. First of all, one observes that the scattering intensity of DNA is much higher than that of the octamer. It is due to the fact that DNA has a higher electronic density. Moreover, NCP and DNA curves present the same minimum

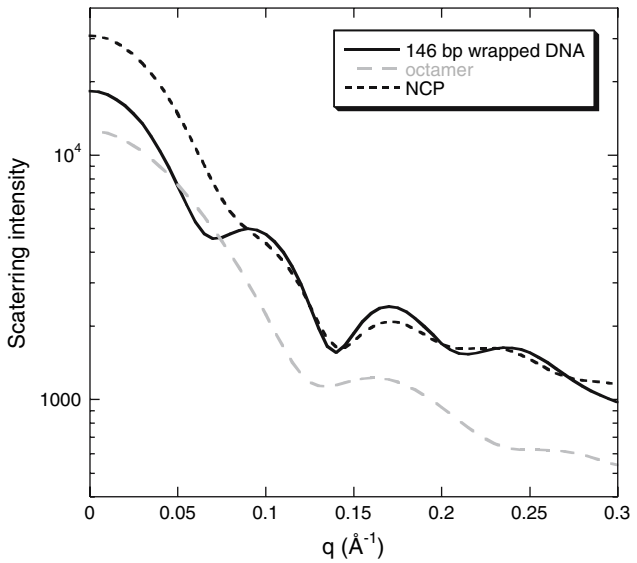

Fig. 7 Comparison of the scattering intensities of the NCP in the crystal (pdb entry 1KX5), the intact octamer, and the 146 bp DNA alone, in the configuration they present in the NCP, wrapped around the histones core. Calculation of the scattering curves was performed with CRYSOL

around $q = 0.14$ Å^{-1}. This minimum in the scattering curve of NCPs is therefore mainly due to the DNA wrapping around the histone octamer. The disappearance of this minimum, experimentally observed for gH2AgH2B NCPs, is the signature of a change in the superhelical path of DNA. At least two processes can be considered to perturb the regular DNA superhelix. The first one is a detachment of the DNA ends from the histone octamer. The second one is an increase of the DNA superhelical pitch. This would be a consequence of the two histone dimers slightly detached from the octamers, drifting apart from the central tetramer. Both alternatives would induce conformational changes that could be detected with SAXS. Simulations of the scattering intensities were performed by taking into account each of these changes: (1) interactions between the histone core and about 25 bp DNA on one side of the entry/exit DNA point or 15 bp on both entry/exit points have been suppressed and (2) the two DNA turns have been separated by a few angstroms in such a way that the symmetry axis of the NCP is lost. The different configurations and the calculated form factors are displayed on Fig. 8. In the first case, a decrease of the minimum amplitude located around $q \approx 0.14$ Å^{-1} is observed, and the simulated scattering intensity is similar to the experimental one. In the second case, the scattering curve is also affected in the same manner around $q \approx 0.14$ Å^{-1}, but it is more difficult to reproduce exactly the experimental curve. SAXS experiments are not able to discriminate between these two mechanisms, but we can attest that the regular DNA wrapping around the histone core is disrupted in gH2AgH2B NCPs. The MNase digestion experiments provide an additional evidence indicating that DNA wrapping is altered in gH2BgH2A nucleosomes.

These two types of modifications are reasonable when considering the locations of the H2A and H2B missing tails. Indeed, the ten C-terminal amino acids of gH2A (118–128) are very close to the two ends of DNA in the crystal structure, and suspected to interact with them in solution. In their absence, one or both DNA ends are likely to unravel from the core. Besides, due to their location between the two turns of the DNA superhelix, it is likely that the positively charged N-terminal H2B tails induce an increase of the electrostatic repulsions between the two superhelical turns of the DNA that lead to an average slightly larger distance between the two DNA turns (Sivolob et al. 2003).

We may wonder whether NCPs whose tails have been deleted after reconstitution are identical or not to NCP reconstituted from globular proteins. There is no way to compare experimentally the two types of particles since a selective deletion of some particular tails after refolding the core from intact histones is not possible. It is only possible to delete all tails by using trypsin or clostripain. SAXS

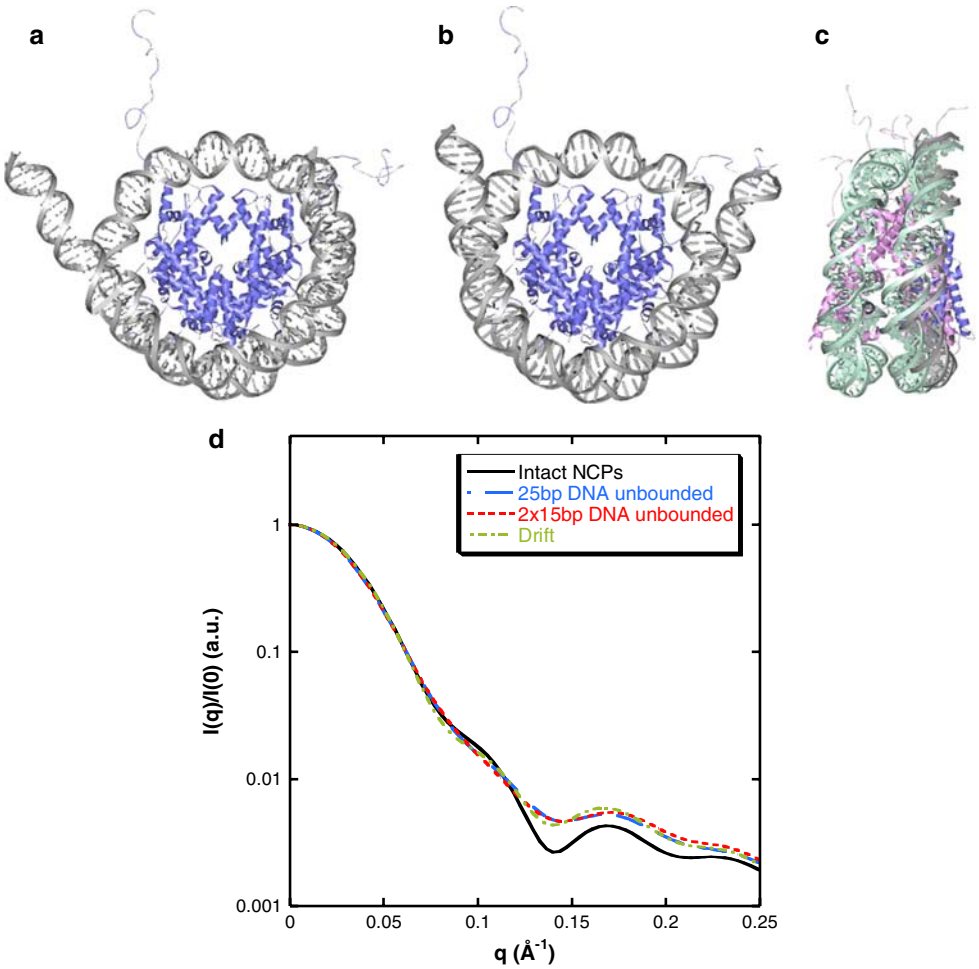

Fig. 8 Possible distortions of the NCP structure (1KX5) seen from *top* (**a**, **b**) and *side* (**c**) views, with their corresponding form factors calculated with CRYSOL (**d**), that could account for the conformation of the gH2AgH2B NCPs. In **a** 25 bp DNA from one end are unbound from the histone core. In **b** 15 bp on both sides of the DNA entry/exit points are detached from the core. In **c** the two histone dimers are drifted by a few angstroms from the tetramers. The new conformation is only slightly different from the initial one. The minor differences can be seen when the two structures are superimposed. (*Blue* and *gray* versus *green* and *purple* for the online color version)

experiments with native NCPs extracted from calf thymus showed how the minimum of the scattering curve at $q = 0.14$ Å^{-1} was decreased upon deletion of all tails by trypsin (Bertin et al. 2004). The authors concluded that the trypsin-digested native NCP is less distorted than the gH2AgH2B recombinant NCP. This distortion may be related to the observation by Dumuis-Kervabon et al. (1986) that clostripain-digested NCPs keep their geometrical conformation. Both results suggest that the tail deletion after reconstitution produces less pronounce effect than the deletion before reconstitution, leading to the conclusion that the H2A and H2B tails play some role in stabilizing the histone core before rewinding DNA. Another approach using Monte Carlo simulations, may also bring some clues. Roccatano et al. (2007) investigated the influence of the tails, by comparing intact and tail deleted NCPs using the 1KX5 PDB file. Increased mobility of both DNA ends was observed as well as a small increase of R_g, coming from a slight increase of the superhelical pitch of DNA, as shown in our experiments. These conformational changes are qualitatively in agreement with our results, but effects are less important probably because the tails are removed after and not before NCP reconstitution.

Role of the tails in DNA-histones interaction and positioning

The alteration of tetramer-dimers and/or DNA-histone interactions would explain why gH2AgH2B NCPs are sensitive to any mechanical treatment. During preparation of the 50 nm thick film for cryo-EM, the high surface tension forces within the film can stretch long molecules such as DNA. These forces have usually no visible effect on colloidal particles such as intact NCPs (Fig. 3b). However, the gH2AgH2B NCPs are highly distorted (Fig. 3a) and their shape in the film is completely different from their conformation in solution. Dissociation of DNA from the core can be complete (as free DNA is often seen) but intermediate steps of the dissociation are also trapped (Fig. 3a). They reveal that at least part of the proteins can be moved along the 147 bp DNA segment up to their end.

Hamiche et al. (2001) have reconstituted NCPs on 256 and 357 bp 5S DNA templates to study the role of histone tails on nucleosome sliding induced by NURF remodeling factors. They unexpectedly found out that upon removal of H2B tails, a nucleoprotein reconstitution artefact is formed and that uncatalyzed nucleosome sliding occurs. They conclude that H2B histone tails are essential for maintaining translational positions of histone octamers on DNA templates. It does therefore imply that affinity of 5S DNA with histone octamers depleted of H2B histone tails is reduced. The 5S DNA sequence used here might not be the most appropriate sequence to achieve particle reconstitution using H2A and H2B tailless histones. A more positioning sequence displaying higher affinity for histones has already been used in that purpose (Dorigo et al. 2003) for the reconstitution of NCPs arrays. In addition to that, Yang et al. (2007) have shown that histone tail affect DNA positioning around NCPs in a sequence dependent manner. They propose that high affinity DNA sequences may mask histone tail contribution to the interaction between DNA and histones. They did not discriminate specifically the histone tails or the tails combination that would be more involved in histone–DNA interactions since all the tails were removed upon trypsin digestion. However, based on our data, we claim that H2A and H2B histone tails are more likely responsible for establishing histone–DNA interactions.

We may wonder if they are also responsible for the different sedimentation coefficients measured on intact, gH3gH4 and gH2AgH2B 12-mer NCPs arrays. In low salt conditions, when arrays are decondensed, sedimentation coefficients are measured to be 27S for gH2AgH2B NCPs, 28.5S for gH3gH4 NCPs and 29S for intact NCPs. Sedimentation coefficients for intact and gH3gH4 NCPs arrays are therefore quite close while gH2AgH2B NCPs arrays come up with a significant lower value. Tse and Hansen (1997) propose that H2A and H2B tails would stabilize the wrapping of the core DNA near the entry-exit point of nucleosomes. Their findings are in good agreement with our own observations.

As a conclusion, we have demonstrated that H2A and H2B histone tails are necessary to properly reconstitute nucleosome core particles. The absence of these histone tails leads to conformational changes of the histone core compared with the intact one. This change induces a deformation of the DNA superhelix.

Acknowledgments The authors would like to thank J.S. Pedersen for his help and advices on the Nanostar in Arhus, D. Svergun and M. Rössle for their technical support on the X33 beamline. We thank Karolin Luger and the Luger lab for the histones plasmids gifts and for sharing their expertise in nucleosome reconstitution and purification. We thank Amélie Leforestier for the EM training and Gerard Pehau-Arnaudet for his help and advices in using the federative 200 kV JEOL FEG 2010 EM located at the Institut Pasteur, Paris. Aurélie Bertin was supported from CNRS fellowship (Centre National de la Recherche Scientifique) and from ARC (Association pour la Recherche sur le Cancer). This work was supported by ANR-06-BLAN-0195-01.

References

Ausio J, van Holde KV (1989) Use of selectively trypsinized nucleosome core particles to analyse the role of histone tails in the stabilisation of the nucleosome. J Mol Biol 206:451–463

Bertin A, Leforestier A, Durand D, Livolant F (2004) Role of histone tails in the conformation and interactions of nucleosome core particles. Biochemistry 43:4773–4780

Bertin A, Renouard M, Pedersen JS, Livolant F, Durand D (2007) H3 and H4 histone tails play a central role in the interactions of recombinant NCPs. Biophys J 92:2633–2645

Brower-Toland B, Wacker DA, Fulbright RM, Lis JT, Kraus WL, Wang MD (2005) Specific Contributions of histone tails and their acetylation to the mechanical stability of nucleosomes. J Mol Biol 346:135–146

Chantalat L, Nicholson JM, Lambert SJ, Reid AJ, Donovan MJ, Reynolds CD, Wood CM, Baldwin JP (2003) Structure of the histone-core octamer in KCl/phosphate crystals at 2.15 angstrom resolution. Acta Crystallogr Sect D Biol Crystallogr 59:1395–1407

Cheung WL, Briggs SD, Allis CD (2000) Acetylation and chromosomal functions. Curr Opin Cell Biol 12:326–333

Clapier CR, Langst G, Corona DFV, Becker PB, Nightingale KP (2001) Critical role for the histone H4 N terminus in nucleosome remodeling by ISWI. Mol Cell Biol 21:875–883

Cosgrove MS, Wolberger C (2005) How does the histone code work? Biochem Cell Biol 83:468–476

Davey CA, Sargent DF, Luger K, Maeder AW, Richmond TJ (2002) Solvent mediated interactions in the structure of the nucleosome core particle at 1.9 A resolution. J Mol Biol 319:1097–1113

Dong F, Nelson C, Ausio J (1990) Analysis of the changes in the structure and hydration of the nucleosome core particle at moderate ionic strengths. Biochemistry 29:10710–10716

Dorigo B, Schalch T, Bystricky K, Richmond T (2003) Chromatin fiber folding: requirement for the histone H4 N-terminal tail. J Mol Biol 327:85–96

Dumuis-Kervabon A, Encontre I, Etienne G, Jaureguiadell J, Mery J, Mesnier D, Parello J (1986) A chromatin core particle obtained by selective cleavage of histones by clostripain. EMBO J 5:1735–1742

Dyer PN, Edayathumangalam RS, White CL, Bao YH, Chakravarthy S, Muthurajan UM, Luger K (2004) Reconstitution of nucleosome core particles from recombinant histones and DNA. Method Enzymol 375:23–44

Eickbush TH, Godfrey JE, Elia MC, Moudrianakis EN (1988) H2a-specific proteolysis as a unique probe in the analysis of the histone octamer. J Biol Chem 263:18972–18978

Fletcher TM, Hansen JC (1995) Core histone tail domains mediate oligonucleosome folding and nucleosomal DNA organization through distinct molecular mechanisms. J Biol Chem 270:25359–25362

Garcia-Ramirez M, Dong F, Ausio J (1992) Role of the histone tails in the folding of oligonucleosomes depleted of histone H1. J Biol Chem 267:19587–19595

Gordon F, Luger K, Hansen JC (2005) The core histone N-terminal tail domains function independently and additively during salt-dependent oligomerization of nucleosomal arrays. J Biol Chem 280:33701–33706

Hamiche A, Kang JG, Dennis C, Xiao H, Wu C (2001) Histone tails modulate nucleosome mobility and regulate ATP-dependent nucleosome sliding by NURF. Proc Natl Acad Sci USA 98:14316–14321

Karantza V, Freire E, Moudrianakis EN (2001) Thermodynamic studies of the core histones: stability of the octamer subunits is not altered by removal of their terminal domains. Biochemistry 40:13114–13123

Konarev PV, Volkov VV, Sokolova AV, Koch MHJ, Svergun DI (2003) PRIMUS: a Windows PC-based system for small-angle scattering data analysis. J Appl Crystallogr 36:1277–1282

Krajewski WA, Ausio J (1996) Modulation of the higher-order folding of chromatin by deletion of histone H3 and H4 terminal domains. Biochem J 316:395–400

Luger K, Mader AW, Richmond RK, Sargent DF, Richmond TJ (1997a) Crystal structure of the nucleosome core particle at 2.8 angstrom resolution. Nature 389:251–260

Luger K, Rechsteiner TJ, Flaus AJ, Waye MMY, Richmond TJ (1997b) Characterization of nucleosome core particles containing histone proteins made in bacteria. J Mol Biol 272:301–311

Mangenot S, Leforestier A, Vachette P, Durand D, Livolant F (2002) Salt-induced conformation and interaction changes of nucleosome core particles. Biophys J 82:345–356

Meersseman G, Pennings S, Bradbury EM (1992) Mobile nucleosomes: a general behavior. EMBO J 11:2951–2959

Noll M (1974) Internal structure of the chromatine subunit. Nucleic Acids Res 1:1573–1578

Pedersen JS (2004) A flux- and background-optimized version of the NanoSTAR small-angle X-ray scattering camera for solution scattering. J Appl Crystallogr 37:369–380

Pennings S, Meersseman G, Bradbury EM (1991) Mobility of positioned nucleosomes on 5-SRdna. J Mol Biol 220:101–110

Petoukhov MV, Svergun DI (2005) Global rigid body modeling of macromolecular complexes against small-angle scattering data. Biophys J 89:1237–1250

Placek BJ, Gloss LM (2002) The N-terminal tails of the H2A–H2B histones affect dimer structure and stability. Biochemistry 41:14960–14968

Pollard K, Samuels ML, Crowley KA, Hansen JC, Peterson CL (1999) Functional Interaction between GCN5 and polyamines: a new role for core histone acetylation. EMBO J 18:5622–5633

Protacio RU, Li G, Lowary PT, Widom J (2000) Effects of histone tail domains on the rate of transcriptional elongation through a nucleosome. Mol Cell Biol 20:8866–8878

Richmond TJ, Searles MA, Simpson RT (1988) Crystal of a nucleosome core particle containing defined sequence DNA. J Mol Biol 199:161–170

Roccatano D, Barthel A, Zacharias M (2007) Structural flexibility of the nucleosome core particle at atomic resolution studied by molecular dynamics simulation. Biopolymers 85:407–421

Sivolob A, Lavelle C, Prunell A (2003) Sequence-dependent nucleosome structural and dynamic polymorphism. Potential involvement of histone H2BN-terminal tall proximal domain. J Mol Biol 326:49–63

Smith RM, Rill RL (1989) Mobile histone tails in nucleosomes. Assignments of mobile segments and investigations of their role in chromatin folding. J Biol Chem 264:10574–10581

Svergun DI (1992) Determination of the regularization parameter in indirect-transform methods using perceptual criteria. J Appl Crystallogr 25:495–503

Svergun D, Barberato C, Koch MHJ (1995) CRYSOL: a program to evaluate X-ray solution scattering of biological macromolecules from atomic coordinates. J Appl Crystallogr 28:768–773

Tse C, Hansen JC (1997) Hybrid trypsinized nucleosomal arrays: identification of multiple functional roles of the H2A/H2B and H3/H4 N-termini in chromatin fiber compaction. Biochemistry 36:11381–11388

Yang ZY, Zheng CY, Thiriet C, Hayes JJ (2005) The core histone N-terminal tail domains negatively regulate binding of transcription factor IIIA to a nucleosome containing a 5S RNA gene via a novel mechanism. Mol Cell Biol 25:241–249

Yang Z, Zheng C, Hayes JJ (2007) The core histone tail domains contribute to sequence-dependent nucleosome positioning. J Biol Chem 282:7930–7938